Implementation of Signal Processing Methods in a Structural Health Monitoring (SHM) System based on Ultrasonic Guided Waves for Defect Detection in Different Materials and Structures

Nekane GALARZA[1], Benjamín RUBIO[1], Alberto DIEZ[1], Fernando BOTO[1], Daniel GIL[1], Jokin RUBIO[1], Eduardo MORENO[2]

[1] Industry and Transport Division, Tecnalia Research & Innovation. Leonardo Da Vinci, 11 Miñano 01510 (Araba) SPAIN nekane.galarza@tecnalia.com
[2] Departamento de Física Aplicada, ICIMAF, 15 No 551, Vedado La Habana, CUBA

Key words: Signal Processing Methods, Lamb waves, Love waves, PZT transducers

Abstract

The local defect inspection in longitudinal structures such as plates or pipelines implies high economical costs and it is time consuming mainly in underground infrastructures, energy or water, and aerospace sectors. Moreover, if these structures are non-accessible, their local inspection is not possible. Ultrasonic (US) inspection technique based on guided waves is one of the potential alternatives to address this issue. The US inspection based on these type of waves could be applied in many scenarios to monitor the damage state of structures; i.e., in water underground pipelines to identify the wall thickness losses or impact damage detection on Carbon Fiber Reinforced Composites (CFRC).

A SHM system based on guided waves requires a special signal processing in order to identify possible damage in the structure. The signal emitted and received is a combination of different propagation modes which are difficult to identify and analyse. However, if the signals are compared to each other (signal related to non-damaged components compared to damaged signal) it is possible to measure their difference as a distance that can be used to estimate the damage level.

In this work, signals corresponding to non-damaged samples have been captured and then different types of damage have been applied for different cases. After the data acquisition phase, the comparison between signals has been carried out by applying different mathematical methods and distance metrics (SDC, DTW, Euclidean, Manhattan and Chebyshev), with the aim of detecting defects in different structures and materials. For this purpose, two cases have been analysed: 1) In CFRC plates subjected to impact damage and deformations and 2) In a pipe coated by cement-mortar in order to quantify the wall thickness losses.

In both cases ultrasonic PZT sensors, an ultrasonic multichannel pulser/receiver and a software developed ad-hoc have been used. Although the SHM system components were similar, it must be noted that the type of ultrasonic guided waves used were different; in the case of CFRC plates, Lamb waves were excited whereas in the case of the pipeline, Love waves have been used. A comparison between the above mentioned methods is provided. The results show the validity of the approach for damage characterization.

1 INTRODUCTION

The aim of the SHM is the identification of changes in different structures (aerospace, civil and mechanical engineering infrastructures) by using a sensor network which checks the condition of the structure periodically, obtaining a continuous, real-time and smart control of the structure. This allows to early detect damages and anomalies, which is motivated by the potential life-safety and economic impact of this technology [1].

In the case of civil infrastructures, there is a special concern about water supply network; population growth (projected to reach over 8 billion in 2030 [2]) and the ageing of pipelines (many built more than 50 years ago [3]), requires the expansion and the restoration of existing water systems; i.e. in America, this will cost $1 trillion over the next 25 years [3].

Regarding the aerospace sector, according to Airbus and Boeing forecasts, the market value is expected to reach up to $4.7-$5.6 trillion (this means the delivery of 31,741-38,050 aircrafts [4, 5]). Thus, the failure of any component would impact the safety of millions of passengers.

Considering the impact, both economical and personal, that the failure of these components would have; this work addresses the implementation of signal processing methods in a SHM system based on ultrasonic guided waves to detect structural changes in composite materials and pipes. The work is divided in 4 sections; the first one describes the fundamental basis of guided waves and the proposed signal processing methods. In Sections 3 and 4 experiments and results are presented, whereas the conclusions are described in Section 5.

2 GUIDED WAVES AND SIGNAL PROCESSING METHODS

Ultrasonic guided waves are a type of waves that can propagate in structures whose perpendicular dimensions to propagation direction are finite (i.e., perpendicular dimensions and wavelength are in the same order of magnitude) such as plates, rods or pipes. Interesting features of these waves are their long-distance propagation through the structure and the size of affected area, larger than in the case of local inspection techniques. These features make the use of guided waves a suitable inspection alternative to be implemented in SHM systems. Pipelines for water supply and several components of aircrafts, mainly composite parts, can be considered as longitudinal or flat structures; so, they could be inspected by using guided waves.

Lamb waves or Shear-Vertical (SV), are a type of elastic guided waves that can propagate through plates [6] and can be mathematically described from two fundamental propagation modes; symmetric and anti-symmetric [7] (Figure 1). The main difference between them is the vibrational motion of the solid particles in the thickness of the plate.

Several research works are focused on the use of these types of waves to inspect CFRC plates for aircraft parts. For example, Z. Su et al. [8], C. J. Lissenden et al. [9] or K. Diamanti et al. [10], have studied the use of Lamb waves due to their capability to inspect large structures, the sensitivity to multiple type of defects (both internal and external) and the use of relatively low-cost devices. The most common type of damages is caused by impact; which can cause matrix cracking, delamination and broken fibres reducing significantly the structure's strength and fatigue life [11]. However, to a lesser extent, there are also studies focused on the identification of the deformation. Considering these studies, this work is based on the identification of impact damage and deformation in composites.

Love Waves are another type of elastic guided waves horizontally polarized (SH), which can propagate through plates "welded" to an elastic half space on one side and vacuum on the

other [12]. In practice, a most realistic approximation of these waves can be considered: a thick plate as the half space, and a gas, like air, as the vacuum (Figure 1).

Love waves are used in many fields of science and technologies such as geophysics, seismology and earthquake engineering. All these applications are based on the main property of Love waves, that any disturbance in the "welded surface" involves a change in boundary conditions and, as a result, a change in the wave propagation. Based on this effect, a recent study carried out by P. Kielczynski et. al [13] is focused on the use of Love waves to study the physical properties of inhomogeneous graded materials.

Considering the pipelines used in water distribution (iron pipes coated with cement-mortar), the coated part can be considered as a "welded" layer that can disturb the wave propagation through the pipe. The thickness loss of this coating may change the properties of the wave, so in this study the use of a realistic approximation of the Love waves is considered in order to identify the progressive coating loss.
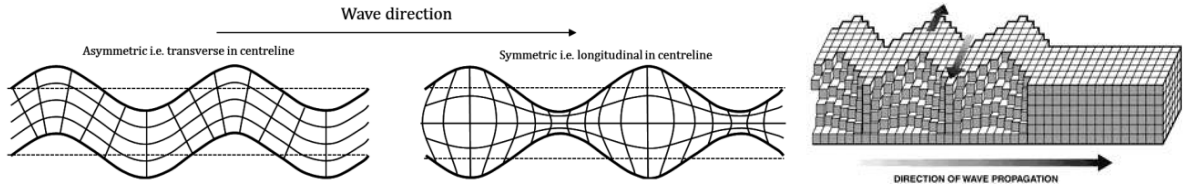

Figure 1: (Left) Lamb waves modes. (Right) Love waves.

Regardless of the type of wave, even though the inspected area is higher than in the case of local techniques, the main drawback when using guided waves consists on the difficulty in the analysis of the collected data. The signals are usually a complicated combination of different propagation modes, such as mode conversion, echoes bouncing from lateral boundaries, etc. The resulting signal is difficult to identify, analyse and, specially, associate to a causative damage, especially in real structures. However, if the collected signals are compared to each other (signals before damage with signals after structural changes) it is possible to estimate their degree of similarity as a mathematical distance, and thus it can be used to quantify the anomaly score [1, 14].

In this work different similarity measurement methods have been applied in order to compute the distance among signals. When two signals are equal their distance will be zero, which means that they are completely similar. The larger difference or distance between two signals yields less similarity [15]. Given two signals $x = (x_1, x_2 \dots, x_n)$ and $y = (y_1, y_2 \dots, y_n)$, where $x_i \in \mathbb{R}$, $y_i \in \mathbb{R}$ and $i = (1, \dots, n)$ distance $d(x, y)$ is calculated on the basis of the following metrics:

- Signal Difference Coefficient (SDC). It computes the distance between signals considering the correlation coefficient between them, as it can be seen in Equation 1:

$$d(x, y) = 1 - \frac{Cov(x, y)}{\sigma_x \sigma_y} \tag{1}$$

Where $Cov(x, y)$ is the covariance of the signals **x** and **y** and σ is the standard deviation.

- Euclidean. It is the most commonly used metric when computing distances. It defines circular regions in Euclidean space, estimating the length of the path connecting each point. The formula is shown as follows (Equation 2):

$$d(\boldsymbol{x}, \boldsymbol{y}) = \|\boldsymbol{x}, \boldsymbol{y}\| = \sqrt{\sum_{i=0}^{n} |x_i - y_i|^2} \tag{2}$$

- Chebyshev. It is also called maximum value distance since it searches for the absolute magnitude of difference between points. Its formulation can be seen in Equation 3:

$$d(\boldsymbol{x}, \boldsymbol{y}) = \max_i |x_i - y_i| \tag{3}$$

- Dynamic Time Warping (DTW). This distance measures the greatest similarity between signals by computing the minimum distance between them in terms of a time warping path. To do so, signals are first aligned. It allows comparing complex signals with shift and stretching of amplitude (Equation 4):

$$d(\boldsymbol{x}, \boldsymbol{y}) = d(n, m)$$

$$d(i, j) = cost(x_i, y_j) + min \begin{cases} d(i, j-1) \\ d(i-1, j) \\ d(i-1, j-1) \end{cases} \tag{4}$$

Where $i = (1, .. n)$, $j = (1, .. m)$ and $cost(x_i, y_j)$ is the cost in aligning the ith element of $\boldsymbol{x} = (x_1, x_2 \ldots, x_n)$ of length n with the jth element of $\boldsymbol{y} = (y_1, y_2 \ldots, y_m)$ of length m for a given distance metric; Manhattan is used in this case (see below) and $n = m$. The final distance is iteratively computed.

- Manhattan. It simply computes the sum of the absolute differences of the Cartesian coordinates at every point x_i and y_i, $i = (1, \ldots, n)$, as it can be seen in Equation 5:

$$d(\boldsymbol{x}, \boldsymbol{y}) = \sum_{i=0}^{n} |x_i - y_i| \tag{5}$$

3 CASE STUDY 1: AEROSPACE SECTOR

In this section, experiments regarding aircraft CFRC components are presented. In the first part materials and methods used are described, whereas in the second part experiments carried out to establish the detection threshold are shown. The last two points are focused on impact damage and deformation experiments.

3.1 Materials and methods

CFRC plates were tested (540x340x2 mm), after bonding two PZT sensors (SML-SP-1/4-0 (Acellent Technologies)) on each. The distance between these transducers was 160 mm. A thermocouple was located in order to monitor the temperature (Figure 2).
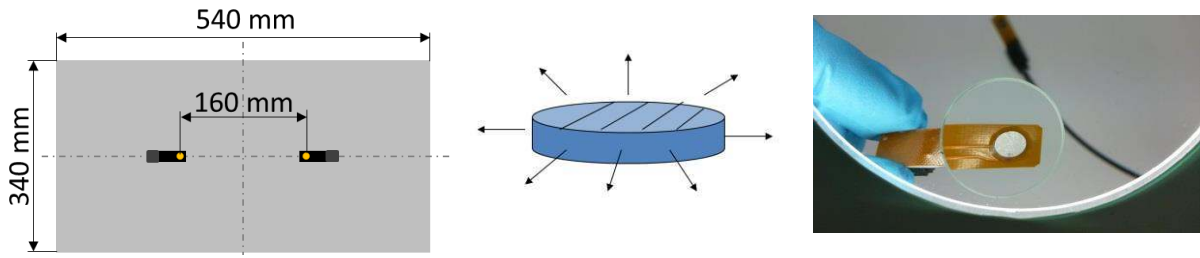
Figure 2: (Left) Scheme of the plate, (Centre) Fundamental radial vibration mode of the PZT, (Right) Detail of the Smart Layer.

Pitch and Catch technique was used, where one of the sensors was the emitter and the opposite one was the receiver. The ultrasonic emission and reception was performed with a multichannel pulser-receiver (SITAU STM-132 (Dasel Sistemas)) and both emission and reception parameters were controlled by using a program developed ad-hoc in Labview^{TM}.

The selection of emission-reception parameters was performed according to the sensor, the characteristics of the electronic and the specimen, as well as the type of guided wave to be excited. In this case, multi-mode (combination of different symmetric and anti-symmetric modes) Lamb waves were generated. The selected frequency range [150 kHz-500 kHz] was centred in the fundamental radial vibration mode of the transducer, 350 kHz-390 kHz (obtained by using an impedance meter (BODE-100 (Omnicron Lab)). The rest of the parameters were; excitation voltage of 40V and 6 burst length signal. The received signal was filtered with a 1 kHz long band-pass filter, centred in the emission frequency.

In all experiments the same steps were followed: signals were acquired doing continuous frequency sweeps [150 kHz-500 kHz] (step 50 kHz), obtaining signals of 8 different frequencies every 5 seconds. This signal acquisition was done before and after the damage, and different mathematical comparison methods were applied to quantify the difference between signals, and hence characterizing damage.

3.2 Estimation of the Detection Threshold

In this work, a comparison between two signals was used as defect detection principle, but there are many factors that could induce a change in a signal that is not related to any anomaly, e.g. the temperature and electronic noise. In order to avoid these false positives, thresholds were established. A threshold is the maximum expected difference between signals corresponding to the same specimen, under the same climatic conditions and the same non-damaged state. Therefore, if any difference between captured signals was higher than its corresponding threshold, it was considered as an anomaly (defect or flexion). On the contrary, any difference below its threshold was considered as "noise". An experimental set-up was defined in order to establish the aforementioned thresholds.

3.2.1 Experimental set-up

The tests were performed at 5±0.5°C and 25±1°C in two different climatic chambers, capturing signals during more than 12h. More than 8500 signals were captured in each case. The sample was covered to isolate it from non-desired airflows (Figure 3).

Once the signals were registered, the first signal captured at the beginning of the experiment was compared with the rest of the signals (signals corresponding to the same temperature, 5ºC or 25ºC, and frequency). The comparison was done by using the different similarity measurement methods described in Section 2. After signal caption, the maximum

value of each mathematical method and frequency was considered between two temperatures and a 30% of safety margin was applied in each case.
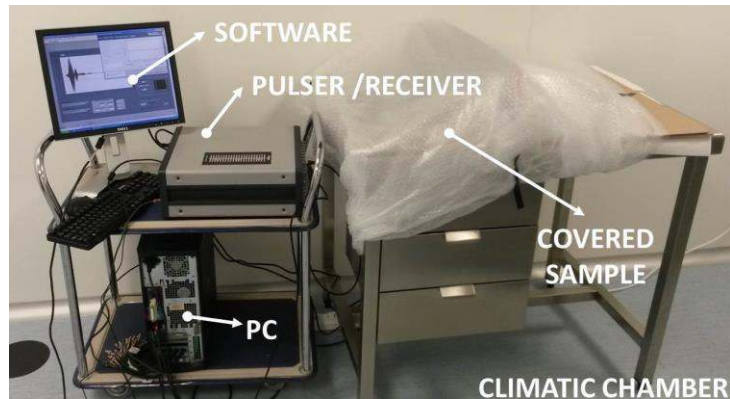

Figure 3: Experimental set-up for thresholds establishment.

3.2.2 Results and conclusions

As can be seen in Figure 5, maximum threshold values were obtained at 400 kHz except for the SDC, in which this maximum was located at 500 kHz.

As an example of changes due to the effect of the temperature and electronic noise, two graphs are presented below (Figure 4) regarding 400 kHz and 500 kHz (at these frequencies maximum and minimum amplitudes were obtained, respectively). It can be seen that at 400 kHz the amplitude change is higher than at 500 kHz, whereas the contrary occurs with the time delay.
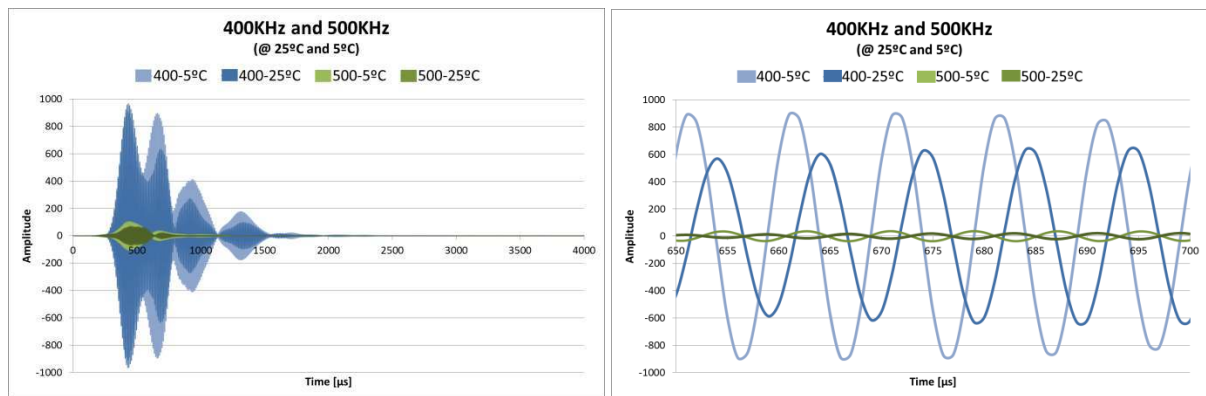

Figure 4: (Left) Signals regarding 400 kHz and 500 kHz captured at both 5 and 25 ºC. (Right) Detail of the signals which shows the effect of the temperature and electronic noise, both in amplitude and time delay.

All methods (except the SDC) are strongly influenced by the amplitude. This means that their results will be higher as long as the amplitude of the compared signals is also higher; thus, the signal changes will be detected easily in that case. Consequently, and regarding results obtained, the higher distances are located between 300 kHz and 450 kHz (around the resonance frequency of the transducers) when the amplitude of the signals is higher (the highest value in both amplitude and threshold is at 400 kHz). At lower frequencies (from 150 kHz to 250 kHz) and at 500 kHz, the amplitudes are lower but similar to each other, then the threshold values are also lower and similar. SDC method is strongly influenced by the phase difference, and therefore the overall values are lower and different from the results obtained by the other distance metrics, as it can be seen in Figure 5.
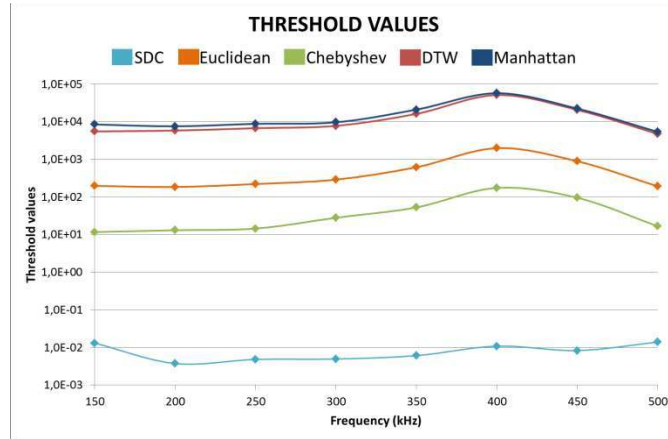
Figure 5: Detection threshold obtained per method.

3.3 Analysis of impact damage

3.3.1 Experimental set-up

The impact tests were carried out with an impact device designed based on the standard AITM1-0010 [16] but adapting it to the specific requirements of the experiments mentioned. This impact device was made up of a steel impactor of 3 kg ($\emptyset_{ext.}$=64 mm/ $\emptyset_{hemisphere}$=20 mm), a steel base and a guided PVC tube (Figure 6).

According to the standard, the first impact energy was 20 J and the rest were 25 J and 40 J. The entire experiment was carried out at constant ambient temperature.

The data acquisition for each impact was; first, capture the data of the plate in non-damaged state during 10 minutes and after the impact during another 10. Damaged material signals were captured after 30 minutes to allow the elastic recovery of the material. Signals regarding the non-damaged state were compared with the signals obtained after the impacts (signals related to the same frequency) by applying the similarity measurement methods described in Section 2. Results and thresholds were normalised in order to equally compare the different metrics. The normalization was done considering the maximum value in each metric. The values above the thresholds were considered as damage and the values below as noise.
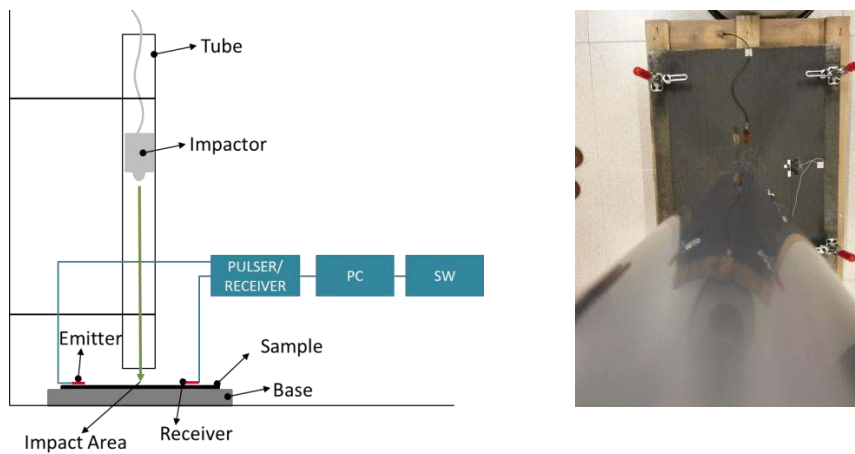

Figure 6: Experimental set-up. Base (ext.670x545 mm/ int.300x500 mm/ e=20 mm), tube ($\emptyset_{int}$=67 mm/ $\emptyset_{ext}$=75 mm/ L=3 m).

3.3.2 Results and conclusions

The results show that 150 kHz is the only frequency in which all similarity measurement methods are able to detect defects for impacts over 25 J, probably because the modes excited are more sensitive to this kind of damages. However, the rest of frequencies and metrics only detect signal changes for impacts over 40 J. At this damage level, probably the structural changes are sufficient, regardless of the excited modes to be detected at every frequency and by all similarity measurement methods. The opposite occurs with defects produced at 20 J; none of the metrics or frequencies is sensitive enough to detect significant changes, most likely because these changes are insufficient to be detected by these methods.

In Figure 7 some samples of signals regarding 25 J for both 150 kHz and 400 kHz are given. At 150 kHz the signal changes in both amplitude and time delay, whereas at 400 kHz mainly the amplitude is affected.
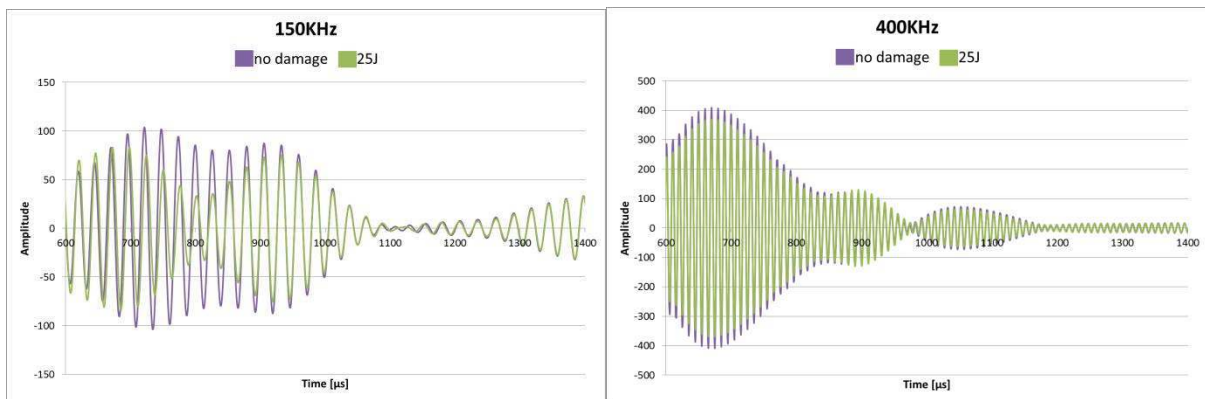

Figure 7: Details of captured signals before and after an impact energy of 25 J. (Left) Changes both in amplitude and time delay can be observed; 150 kHz. (Right) Changes mainly in amplitude are shown; 400 kHz.

In Figure 8 the two most significant results are shown. One graph regards to 150 kHz in which the threshold is exceeded in all metrics after impact energy over 25 J. In regards to the results at 400 kHz, it can be observed that the threshold is exceeded only when an impact of 40 J is applied. Moreover, in this last graph it can also be noted that the obtained values are higher in all metrics (except in SDC), corresponding with the maximum amplitude of signal at this frequency. The rest of the frequencies are not shown because results are similar to those obtained at 400 kHz but with lower normalised values.
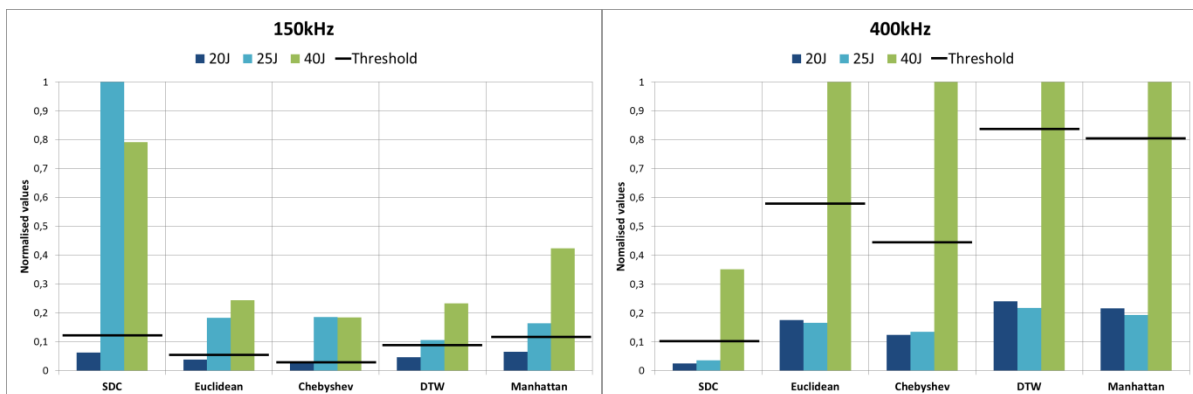

Figure 8: Impact test results at 150 kHz (data related to 25 J and SDC is considered as an outlier) and 400 kHz.

3.4 Analysis of deformation

3.4.1 Experimental set-up

The deformation was applied by using a Universal Testing Machine E1/004 (100KN, Class 1) with a flexion testing tool (Figure 9).

The definition of the deformation levels was established calculating the maximum stress of the material. This value was obtained doing interlaminar shear static tests under ASTM D2344 standard [17]. Considering the results given by these tests, different levels of deformation were established (from 0 to 10 mm with steps of approximately 3 mm). It must be also noted that the plate was bended progressively (bending stage) and then, after the maximum stress, the strength was reduced also progressively in order to obtain also information about a possible hysteresis.

The signals were acquired during approximately 8 minutes in each stage and the signals corresponding to the pattern of the plate without deformation were compared with the signals obtained after the deformations (signals related to the same frequency) by using the different similarity methods described in Section 2.

As in previous experiment, results and thresholds were normalised in order to equally compare the different metrics. The normalization was done considering the maximum value in each metric. The values above the normalised threshold were considered as damage and values below as noise.
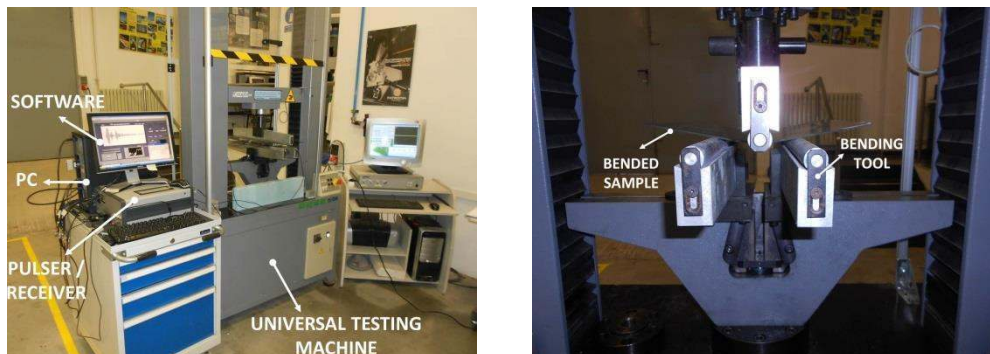

Figure 9: Experimental set-up for deformation testing.

3.4.2 Results and conclusions

According to the results, there is not any especially sensitive frequency to detect deformation for all metrics (sensitivity was obtained from the average slope of the curves presented in Figure 11) and in all deformation levels the threshold values were exceeded.

As it is shown in Table 1, at low frequencies; data regarding 150 kHz show that SDC is the most sensitive in comparison with the rest of frequencies and metrics. Probably this is due to the fact that this frequency promotes the excitation of more sensitive modes to phase changes, which could be directly related to mode conversion generated by the deformation (at 200 kHz the same trend is observed, but the sensitivity of SDC is lower than at 150 kHz). In contrast, at higher frequencies (400 kHz and 450 kHz) the SDC seems to be less sensitive than other metrics (except the DTW at 450 kHz), which obtained similar results among them. A priori, SDC detects these signal changes better when the amplitude of the signal is not very high and at high frequencies the amplitudes are higher than in the rest of cases; which can justify the different detection capability of different metrics. In general, at all frequencies, the

9

DTW is the least sensitive, including at 350 kHz, in which all values are similar except in the case of DTW. These low values could be explained on the basis of the DTW distance computation, which align signals in time to best match shift and stretching of amplitude between signals. Then, it does not consider the phase changes produced by the deformation at certain amplitudes. Finally, 500 kHz seems not to be useful to detect flexion. No significant hysteresis is observed. The hysteresis observed is always less than 5%, for deformation values higher than 2mm.

Two graphs are presented as an example of some captured signals (150 kHz and 500 kHz) As it can be seen in Figure 10, more changes are produced for the same flexion level (≈10 mm) at 150 kHz than at 500 kHz; which is consistent with results obtained.
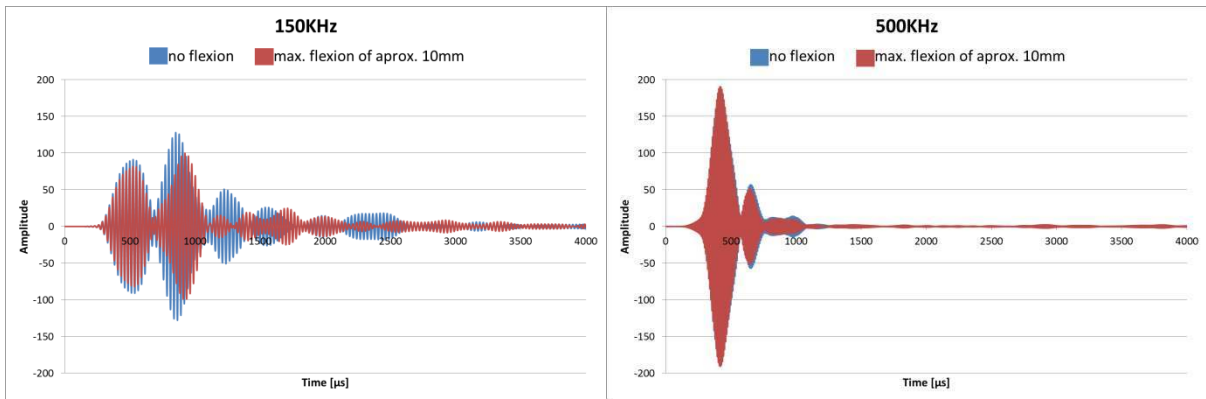

Figure 10: Signals regarding 150 kHz and 500 kHz, respectively. Signal changes are more significative at 150 kHz than at 500 kHz for the same flexion level.
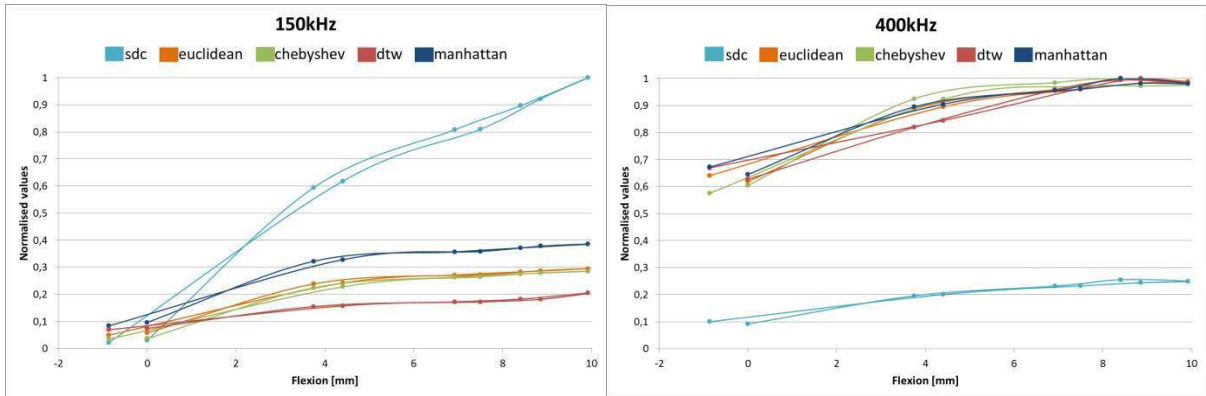

Figure 11: Flexion test results at 150 kHz and 400 kHz (the offset regarding all metrics, except the SDC, are due to the high amplitude of the signals at this frequency).

	150kHz	200kHz	250kHz	300kHz	350kHz	400kHz	450kHz	500kHz
SDC	1,0	0,3	0,58	0,3	0,38	0,17	0,05	-0,01
Euclidean	0,26	0,07	0,39	0,16	0,45	0,39	0,11	-0,01
Chebyshev	0,27	0,04	0,47	0,14	0,56	0,42	0,13	0,01
DTW	0,13	0,05	0,13	0,13	0,15	0,39	0,03	0
Manhattan	0,31	0,11	0,35	0,22	0,38	0,35	0,14	-0,01

Table 1: Sensitivity to deformation of different methods.

4   CASE STUDY 2: ENERGY SECTOR (WATER DISTRIBUTION)

In this section, experiments regarding water distribution pipes are presented. In the first part, materials and methods are described. In the following point, the experiment is described and results obtained are discussed. In this case, detection thresholds are not calculated because the objective is not to establish in which stage is considered the damage, but to determine the tendency of the signal while the coating part is losing its thickness progressively.

4.1 Analysis of thickness loss

4.1.1 Materials and methods

Cast iron pipe coated with cement mortar was tested ($\emptyset_{int}$=204 mm/ $\emptyset_{ext}$=234 mm / e_{coat}=3 mm). The experiment was carried out in half a pipe to be able to induce defects. Three tooth-shaped PZT transducers, designed by Tecnalia, were bonded to the outer face of the pipe. These transducers work in shear mode and they have rectangular PZT elements with polarization vector perpendicular to the direction of the electric field (Figure 12).

The distance between the emitter and the first receiver was of 100 mm and the second receiver was located next to the first one (110 mm from the emitter). The experiment was carried out at constant ambient temperature. The samples tested are shown in Figure 12.
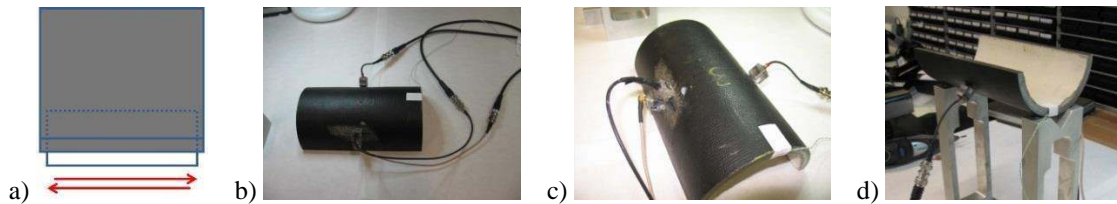

Figure 12: a) Scheme of Tecnalia shear transducers (vibration motion is indicated with arrows). b,c) Outer face of the sample. d) Inner face of the sample.

Pitch and Catch technique was used, where one of the sensors was the emitter and the opposite two were the receivers. The ultrasonic emission and reception was done with a multichannel pulser-receiver (Tecnalia) and the parameters, both emission and reception were controlled by using a program developed ad-hoc in Labview^{TM}.

The emission frequency range was selected around the main shear resonance frequency, 150 kHz [50-300 kHz]. The rest of the emission parameters were; excitation voltage of 350V and 6 burst length signal. The receiver signal was filtered with a 2 kHz long band-pass filter, centred in the emission frequency.

After preparing the samples; first, signals were acquired doing continuous frequency sweeps from 50 kHz to 300 kHz with a step of 50 kHz, obtaining signals of 6 different frequencies. This signal caption was done before and after the damage. Then, similarity measurement methods described in Section 2 were applied to obtain damage information.

4.1.2 Experimental set-up

The simulation of the thickness loss was performed with a drill (Ø8 mm). 14 levels of damage were performed in order to simulate a progressive thickness loss (Figure 13, Table 2).

As in previous experiments, results were normalised in order to compare distances computed by the different metrics used.

Damage	Dimension	Damage	Dimension	Damage	Dimension	Damage	Dimension
D1	10x10x1,5	D5	30x10x1,5	D9	40x33x1,5	D13	Ø8, e=2,7
D2	10x10x3	D6	30x15x3	D10	40x33x3	D14	L=16, e=2,7
D3	20x10x1,5	D7	40x15x1,5	D11	40x45x1,5		
D4	20x10x3	D8	40x15x3	D12	40x45x3		

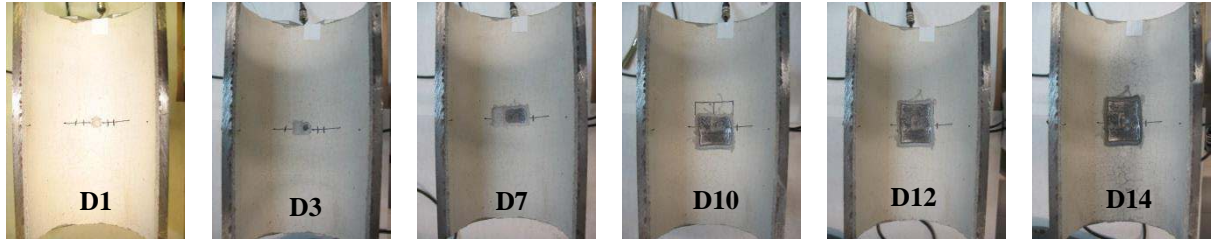Table 2: Sequence of damages and their dimensions (mm).

Figure 13: Some of the induced damages.

4.1.3 Results and conclusions

Low frequencies (50 kHz and 100 kHz) seem to be the most suitable to detect this kind of defects. In these two cases, SDC and DTW seem to be less appropriate. Regarding SDC, although the values are monotonically increasing, the magnitudes are low; this may be caused due to the fact that high amplitude of these signals could "overshadow" the effect of the time delay produced by the damages (Figure 15). On the contrary, the rest of metrics (except DTW) present better ability to detect signal changes at high amplitudes, which is the reason why they detect the defect better at these two frequencies.

In the next Figure 14 it can be seen as an example of signals related to different damages captured at 50 kHz. On the left it is possible to notice the high differences between signals produced by different damages. On the right, it can be observed that in two consecutive damages, the signal difference is not so obvious in comparison with two non-consecutive damages.
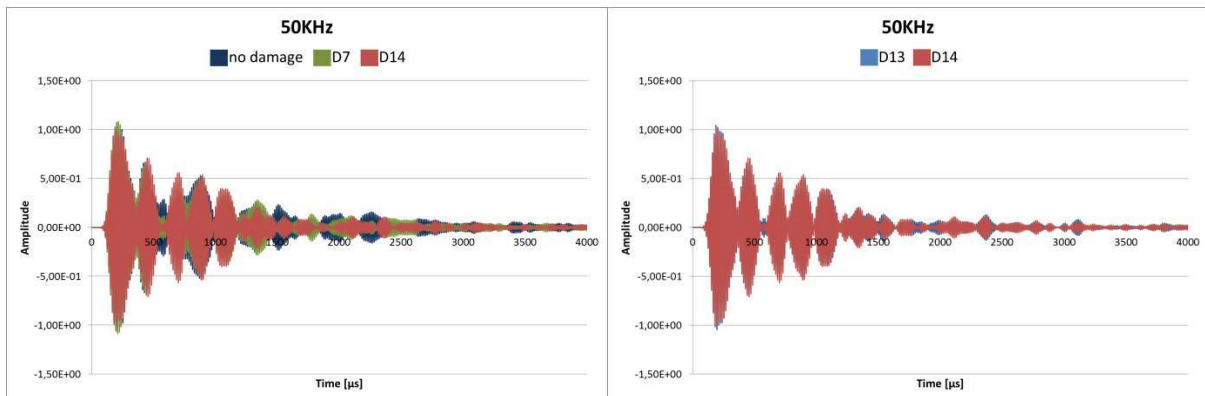

Figure 14: Signals captured at 50 kHz. Note that there are significant changes in non-consecutive defects than in two consecutive.

At high frequencies (250 kHz and 300 kHz) the signal differences are not meaningful except in the case of SDC, but these changes are not strictly monotonous (Figure 15). At 150 kHz and 200 kHz, the changes detected with all metrics do not match the applied damage; hence it can be concluded that these frequencies are not suitable to detect this kind of damages, so no graphs regarding these frequencies are presented. At these frequencies, it

seems that the excited modes are not very sensitive to this kind of defects. There are not significant differences between the two receivers.
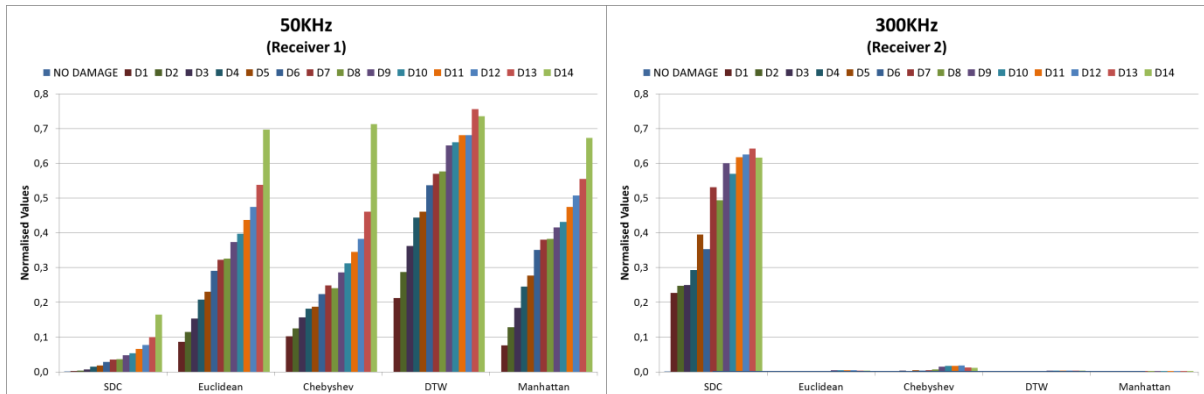

Figure 15: Normalised thickness loss test results at 50 kHz and 300 kHz. At 50 kHz the capability to detect progressive defects is higher than at 300 kHz.

5 GENERAL CONCLUSIONS

In general, according to the results obtained in all experiments, Euclidean, Manhattan and Chebyshev seem to be more effective to detect differences between signals, when their amplitudes are higher. In contrast, the higher the amplitudes, the more "overshadowed" the resolution of SDC.

Analysing the different damages, in impact tests the results show that all metrics are able to detect defects over 40 J instead of at 150 kHz, in which defects induced at 25 J are also detected.

On the other hand, the sensitivity of the different methods in detecting deformation and thickness loss, showed strong correlation with frequency. However, there are frequencies and metrics more likely to detect this kind of damages; for example, at 150 kHz and 200 kHz SDC seems to be the most adequate for deformation detection whereas at 50 kHz and 100 kHz Euclidean, Manhattan and Chebyshev show a better behaviour.

From the point of view of the control unit of a SHM system, the difference between a fluctuating bending (e.g., wings of an aircraft) and a permanent damage (e.g., impact on the fuselage) could be found by analysing the persistence of the change in the signals.

The DTW does not seem to optimally detect damages in this kind of structures and experiments. In order to cover as many types of induced changes of signals as possible, a multiple evaluation using simultaneously SDC and Euclidean or Manhattan methods, may be a more accurate strategy to monitor several structures.

ACKNOWLEDGEMENTS

REFERENCES

[1] C.R. Farrar, K. Worden. An introduction to structural health monitoring. Philosophical Transactions of the Royal Society A. Phil. Trans. R. Soc. A (2007) 365, 303-315. Doi: 10.1098/rsta.2006.1928

[2] Facts and trend, Water. World Business Council for Sustainable Development (WBCSD, August 2005. Reprint March 2006). ISBN 2-940240-70-1

[3] Buried No Longer: Confronting America's Water Infrastructure Challenge. 2011.

[4] Global Market Forecasts. Flying by numbers 2015-2034. Airbus

[5] Current Market Outlook 2015-2034. Boeing

[6] Lamb, H. "On Waves in an Elastic Plate." Proc. Roy. Soc. London, Ser. A 93, 114–128, 1917.

[7] E. Moreno, P. Acevedo. Thickness measurement in composite materials using Lamb Waves. Ultrasonics 35 (1998) 581-586.

[8] Z. Su, L. Ye, Y. Lu. Guided Lamb waves for identification of damage in composite structures: A review. Journal of Sound and Vibration 295 (2006) 753-780

[9] C.J. Liessenden, F. Yan, E.T. Hauck, D.M. Noga, J.L. Rose. Internal damage detection in laminated composite plate using ultrasonic guided waves. Review of Quantitative Nondestructive Evaluation Vol. 26, ed. by Thomson and D.E. Chimenti (2007)

[10] K. Diamanti, J.M. Hodgkinson, C. Soutis. Detection of Low-velocity Impact Damage in Composite Plates using Lamb Waves. Structural Health Monitoring 2004 3: 33. DOI: 10.1177/1475921704041869.

[11] K. Diamanti, C. Soutis. Structural health monitoring techniques for aircraft composite structures. Progress in Aerospace Sciences 46 (2010) 342–352

[12] A.E.H. Love, "Some problems of geodynamics", 1911. Cambridge University Press

[13] P. Kielczynski, M. Szalewski, A. Balcerzak. Propagation of ultrasonic Love waves in nonhomogeneous elastic functionally graded materials. Ultrasonics 65 (2016) 220-227.

[14] H. Gao, Y. Shi and J. L. Rose. Guided Wave Tomography on an Aircraft Wing with Leave in Place Sensors. AIP Conf. Proc. 760, 1788 (2005).

[15] Cha, Sung-Hyuk. "Comprehensive survey on distance/similarity measures between probability density functions." City 1.2 (2007): 1.

[16] AITM1-0010. Fibre Reinforced Plastics. Determination of Compresion Strength After Impact.

[17] ASTM D2344. Standard Test Method for Short-Beam Strength of Polymer Matrix Composite Materials and Their Laminates.